

# Numerical simulation of wind flow around an elastic inflated membrane

Viktor Šajn, Franc Kosel and Boris Štok

Faculty of Mechanical Engineering, University of Ljubljana, Aškerčeva 6, SI-1000 Ljubljana, SLOVENIA  
e-mail: viktor.sajn@fs.uni-lj.si

## SUMMARY

*The aim of this paper is to present a simulation of a turbulent wind flow around an elastic inflated cylindrical membrane. The aeroelastic model consists of a flexible, large-displacement membrane and the Reynolds-averaged Navier-Stokes equation of a stationary flow with the  $k-\varepsilon$  turbulence model. The wind flow around the membrane was simulated as a two-dimensional turbulent flow around a deformable curve fixed at the ends. For simulating the problem, the Finite Element Method (FEM) was used. In the iterative calculation process, the shape of the fluid mesh is adapted to the shape of the solid. This adaptation is made so that in the calculation process of the solid the fluid mesh is taken as a weak, quasi solid. The simulations were performed for wind velocities of 10, 15 and 17.5 m/s and the Reynolds numbers in terms of membrane diameters  $6.7 \cdot 10^6$ ,  $10 \cdot 10^6$  and  $11.8 \cdot 10^6$  with an inflating pressure 100 Pa. The results of the simulation show that the membrane is stable and has an acceptable shape when the ratio between the dynamic pressure of the wind and the inner pressure  $r_p$  is less than 1 and it collapses when this ratio exceeds 2.*

**Key words:** membranes, aeroelasticity, fluid-solid interaction,  $k-\varepsilon$  model of turbulence.

## 1. INTRODUCTION

Inflatable constructions are popular because they can be set up quickly and it is easy to transfer them to another place. They are especially used for covering and heating outdoor sport facilities in winter time. The stabilization of the structure is provided by the inner pressure which carries the membrane of the construction. The building is sealed, the inflated air is a substitute for the lost air. The wind force is the main external force which acts on the inflated membrane. By increasing the inner pressure, the construction becomes more stable and resistant to the wind force but because of a higher stress in the membrane it has to be thicker, and the foundations and attaching points have to be stronger. The main objective of this paper is to present the influence of the wind flow on the deformation of the membrane taking into consideration the inner pressure.

In literature, the study of wind flow influence on the deformable membrane has been mainly focused on

the analysis of membrane airfoils and yacht sails. Cyr and Newman [1] simulated the two-dimensional flow over the membrane airfoil with a potential theory. The separation was simulated by additional vortices whose position was calculated by boundary layer integral equations. This method is still limited with a wind angle of attack being tangential to the leading edge of the sail; hence, the viscous effect from the ground cannot be included. A three-dimensional simulation of a turbulent flow around a downwind sail with separation was made by Hedges, Richards and Mallison [2]. The sail was fixed with no deformation or displacement. A simulation of the flow around a flexible membrane airfoil was carried out by Smith and Shyy [3]. For the turbulence model, SST  $k-\omega$  was used. The reported results present a small rate of membrane displacement. Argyris [4] have performed a numerical simulation of solid-fluid interaction. The coupling was done for moving boundaries and the Euler-Lagrangian formulation of the fluid was used. The low Reynold number simulations were carried out.

## 2. GOVERNING EQUATIONS

The fluid and deformable solid are described with constitutive equations. The description of the coupled solid-fluid system consists of constitutive equations for the fluid and solid with additional equations on the common boundary between the fluid and the solid. For a turbulent flow of the fluid, the Reynolds averaged Navier-Stokes equations written in the Euler form are:

$$\frac{\partial \rho}{\partial t} + (\rho v_i)_{,i} = 0 \quad (1)$$

$$\frac{\partial}{\partial t} (\rho v_i) + (\rho v_i v_j)_{,j} = -p_{,i} + [(\mu + \mu_t) v_{i,j}]_{,j} \quad (2)$$

where  $\rho$  is fluid density,  $v_i$  fluid velocity,  $p$  pressure and  $\mu$  dynamic viscosity of the fluid. For the  $k$ - $\epsilon$  turbulence model, eddy turbulent viscosity  $\mu_t$  is defined with:

$$\mu_t = -\rho C_\mu k^2 / \epsilon \quad (3)$$

where  $k$  is kinetic energy of the turbulence which is defined:

$$\frac{\partial}{\partial t} (\rho k) + (\rho v_j k)_{,j} = -\tau_{ij} v_{i,j} - \rho \epsilon + [(\mu + \mu_t / \sigma_k) k_{,j}]_{,j} \quad (4)$$

The kinetic energy dissipation rate  $\epsilon$  is:

$$\frac{\partial}{\partial t} (\rho \epsilon) + \rho v_j \epsilon_{,j} = C_{\epsilon_1} \frac{\epsilon}{k} - \tau_{ij} v_{i,j} - C_{\epsilon_2} \rho \frac{\epsilon^2}{k} + [(\mu + \mu_t / \sigma_\epsilon) \epsilon_{,j}]_{,j} \quad (5)$$

$$\tau_{ij} = \mu_t (v_{i,j} + v_{j,i}) \quad (6)$$

with closure coefficients.

For the formulation of an isotropic static solid written in the Lagrangian form, the conservation of the moments and rheology equations are considered:

$$\sigma_{ji,j} + \rho f_i = 0 \quad (7)$$

$$\sigma_{ij} = \frac{E}{1+\nu} \left( \epsilon_{ij} + \frac{\nu}{1-2\nu} \delta_{ij} \epsilon_{kk} \right) \quad (8)$$

where  $f_i$  are external forces,  $\sigma_{ij}$  is stress tensor,  $\epsilon_{ij}$  is strain tensor, and  $\nu$  is Poisson number. The strain tensor is calculated from the displacement vector:

$$\epsilon_{ij} = \frac{1}{2} (u_{i,j} + u_{j,i}) \quad (9)$$

where  $u_i$  is displacement vector. In the present application, large displacements are considered because of a high ratio between the membrane length and thickness. Large displacements exert an influence on the solid geometry. This makes the system non-linear and the successive iterative scheme on the deformed geometry has to be used. The strain tensor is still small and the linear Hook's model of deformations, Eq. (8), can be used.

The constitutive equations of the fluid are written in the Euler form and those of the solid in the Lagrangian form. This brings the problem of two different forms of equations to the interface between the fluid and solid. From this it follows that the conservation of momentum in the interface between the fluid and solid [5] can be written as:

$$p^f = -p^s \quad (10)$$

For the solid the pressure is  $p^s = \sigma_{ij} n_j n_i$ . For the fluid flow the solid defines the viscous wall:

$$v_i^f = 0 \quad (11)$$

## 3. NUMERICAL CALCULATIONS

In the numerical modeling of the wind-structure interaction, ABAQUS® and Fidap® numerical software packages were used. ABAQUS® [6] is based on the finite element method and is capable of simulating a large displacement with a small strain. The program successively calculates the equilibrium on the deformed geometry by successively increasing the part of the boundary forces to the full value. For each iteration the stiffness matrix is calculated. Fidap® [7] simulates the turbulent fluid flow based on the  $k$ - $\epsilon$  turbulent model. The fluid flow was considered as stationary and only the diffusion matrices had to be calculated in each iteration step. The interaction between the two programs and the interchange of the coupling boundary conditions were provided with an additional code. For the calculation of the final static equilibrium shape of the solid the iteration process operates with both solvers. In the process of calculating the solid deformation, the fluid domain mesh was represented as a weak, quasi-solid connected to the calculated solid. In this way we ensure a permanent contact between the fluid and solid meshes. The algorithm is presented in Figure 1.

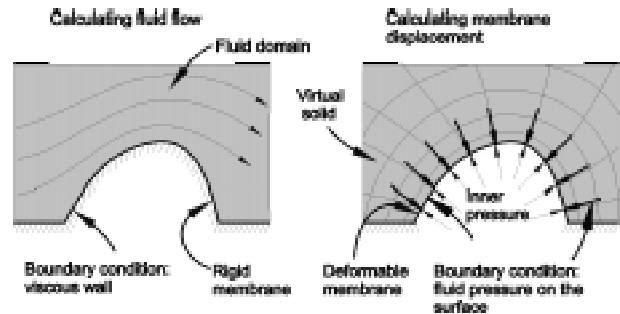


Fig. 1 Numerical algorithm of the fluid-solid interaction

An analysis was made of a stationary, two-dimensional turbulent flow around the deformable solid, particularly of the changes of shapes, fluid forces on the solid and the fluid streamlines around the coupled fluid-solid system. In the calculation of the fluid flow, an interface between the fluid and solid

represents a viscous wall boundary condition. In the calculation of the solid deformation, fluid surface forces on the interface between the fluid and solid represent the loading force acting on the solid.

Specifications of testing conditions are presented in Figure 2. Calculations were performed for a two-dimensional flow around a deformable sail membrane, with a radius  $R=6\text{ m}$ , and inner stabilizing pressure  $p^n=100\text{ Pa}$ . The stiffness of the membrane was  $k=12\cdot 10^6\text{ N/m}^2$ . The air density was  $\rho=1.25\text{ kg/m}^3$  and dynamic viscosity  $\eta=22.22\cdot 10^{-6}\text{ Pas}$ . The calculation was performed for three velocities of the wind  $v=10\text{ m/s}$ ,  $v=15\text{ m/s}$  and  $v=17.5\text{ m/s}$ . The viscous effect of the ground was included by a viscous wall in front of and behind the membrane.

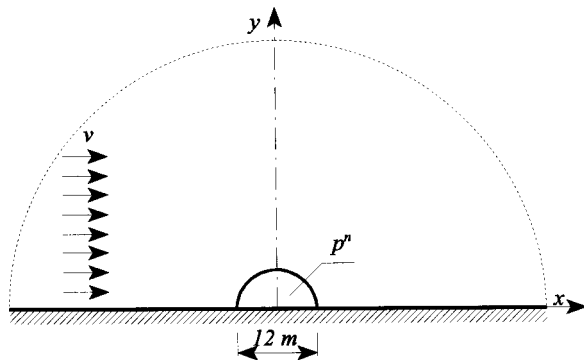


Fig. 2 Definition of the wind flow around the membrane and discretisation area

The finite element mesh of the fluid consists of 1600 quadrilateral plane elements (Figure 3) whose thickness is reduced in the vicinity of the membrane for a proper description of viscous effects. The turbulent boundary layer function is implemented on the fluid elements attached to the membrane and ground. The finite element mesh of the membrane consists of 40 beam elements. An additional mesh of quadrilateral plane elements, geometrically identical to the finite elements of the fluid, is connected to the membrane mesh. The stiffness of the additional mesh is  $10^{-6}$  compared to the membrane so it has a neglecting influence on the deformation of the membrane elements. The displacements of the attached mesh nodes were used for defining the new position of the fluid nodes to ensure permanent contact between the fluid and solid domains. The number of the finite elements and the size of the problem were limited by the computer power and velocity of the network data transfer.

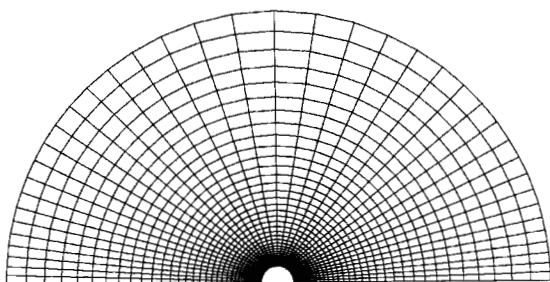


Fig. 3 Finite element mesh of the discretisation domain

The velocity and pressure were fixed on the open side of the interface of the fluid domain. The viscous wall boundary condition was defined on the ground and on the membrane. The membrane had a fixed displacement of last nodes. The computing procedure consisted of calculating the fluid flow with a defined area. For the first calculation the boundary values were taken as initial on the nodes. A code developed by the research team recalculated the node forces from the fluid pressure and applied them to the solid as a boundary condition. With another code, the calculated node displacements of the attached mesh were used for generating a new fluid mesh. In the next iteration, the initial nodes values were taken from the previous iteration cycle. For the convergence condition, the change of the resulting force from the fluid to the membrane was observed.

#### 4. RESULTS OF THE SIMULATION

Separate workstations were used for the fluid and solid calculations. The developed code ensured communication between workstations and solvers. The time required for one complete calculation was approximately 5 hours, considering that the solvers were working in sequences. In the process there was no problem of convergence with the fluid flow simulation. On the other hand, a big difference between the stiffnesses of the areas in the solid led to a poor pivot of the stiffness matrix. The starting time step of the force had to be lowered to  $10^{-6}$  regarding the complete force because the solid had a displacement which was too large on the first increment and the convergence could not be obtained. Figure 4 presents the resulting force from the fluid to the membrane with iteration cycles. The membrane equilibrium and the stationary fluid flow are achieved in less than 10 iteration cycles with the convergence criteria difference between sequence iteration less than  $10^{-3}$ .

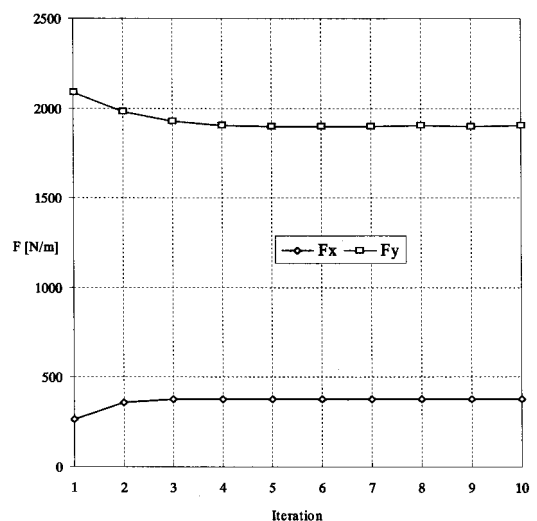


Fig. 4 Convergence of the resulting forces components on the membrane supports

The simulations were provided for velocities of 10, 15 and 17.5 m/s. For the evaluation of the results we defined the pressure ratio between dynamical forces and inside pressure:

$$r_p = \frac{\rho v^2}{2 p^n} \quad (12)$$

where the velocities were considered far away from the membrane.

**Case 1**

Figure 5 represents a velocity field of incompressible viscous flow around the deformable membrane in statical equilibrium. The fluid velocity far away from the membrane is 10 m/s and the pressure ratio is 0.625. The maximal velocity is 15.37 m/s and the highest point of the membrane is moved by 0.47 m downstream horizontally and by 0.91 m upward regarding the no wind equilibrium state. On the back side of the membrane there is an area of high velocity drop near the membrane from 10 m/s to 3 m/s. Separation occurs in this area.

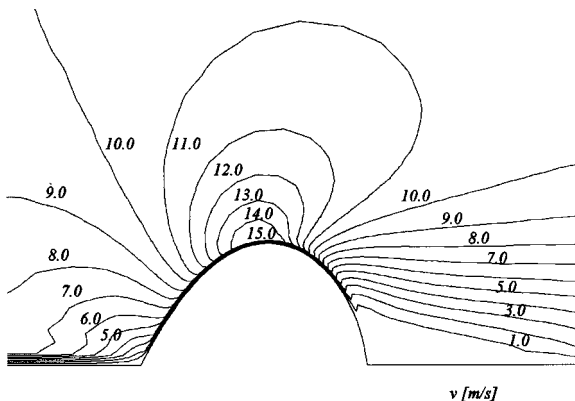


Fig. 5 Contour lines of constant velocity for free stream velocity v=10 m/s

**Case 2**

For a wind speed 15 m/s, Figure 6, the top of the membrane in statical equilibrium is moved by 1.78 m horizontally downstream and by 0.54 m upward. The pressure ratio is 1.407 and the maximal velocity of the air is 22.7 m/s. Separation of the flow occurs in the same area with a higher velocity gradient.

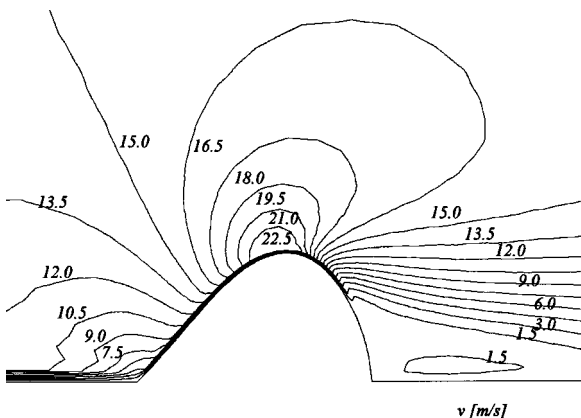


Fig. 6 Contour lines of constant velocity for free stream velocity v=15 m/s

**Case 3**

Figure 7 presents the velocity flow field for velocity of 17.5 m/s. The pressure ratio is 1.914. The membrane highest point is lowered compared to the second case by 2.54 m downstream horizontally and by 0.48 m upward vertically regarding the no wind case. It was found that the membrane collapses for the wind speed of 20 m/s around the deformable membrane which means a pressure ratio of 2.5.

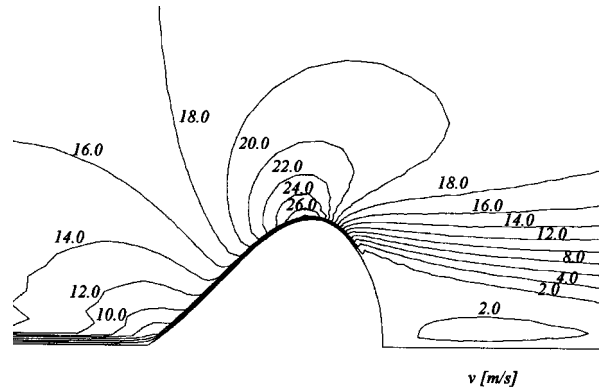


Fig. 7 Contour lines of constant velocity for free stream velocity v=17.5 m/s

**Discussion**

Figure 8 presents the components of the reactions to the foundations from the inner pressure and wind pressure for the deformed and rigid membrane. For the nowind case, only the vertical component exists because of the cylindrical test shape of the membrane. For the deformed membrane the vertical force for case 3 is smaller than that for case 2 which has the same trend as observed from the movement of the highest point of the deformable membrane. This is opposite to the resulting force for a rigid membrane where both horizontal and vertical forces increase with the wind velocity. The vertical resulting force on the deformable membrane is 8.8 % smaller for case 1, 29.7 % for case 2 and 46.1 % for case 3 compared to the rigid membrane vertical forces for the same case. The horizontal force for the deformable membrane is greater compared to the rigid membrane force and is 42.7 %, 68.6 % and 75.1 % greater for the each of cases, respectively. The reason for increasing the horizontal force is in the shape of the deformed membrane which has a conspicuous back part in which a strong whirl is produced.

Figure 9 presents the curves of the statical equilibrium shape membrane and the resulting forces in the support. For case 1 the curvature of the upwind part of the membrane is from the same side as for no wind case. For cases 2 and 3 the front part of the membrane has an opposite curvature compared to the initial one. For the same cases, the difference between the first and second resulting force in the support is a result of the numerical error and it can be estimated as less than 1 %. The wind force and the inner pressure forces act normally to the membrane curve and do not accumulate axial force along the curve. The absolute

values of the reaction forces on both supports have to be equal. The direction of the reaction force vector of the rear support changes slightly which differs from the front support reaction force where the horizontal component is increasing with the wind velocity. The increase of the support reaction forces with excluded reaction force to the inner pressure is not linear with the pressure ratio. If we compare the reaction forces which are a consequence of the wind for the rigid shape and the deformable membrane we find that reactions of the supports are by 13.8 % smaller for the case 1 compared to the rigid membrane. For case 2, they are by 33.3 % and for case 3 even by 45.9 % smaller than those of the rigid membrane for the same test conditions. This proves that the deformable membrane adapts its shape to decrease the reacting forces.

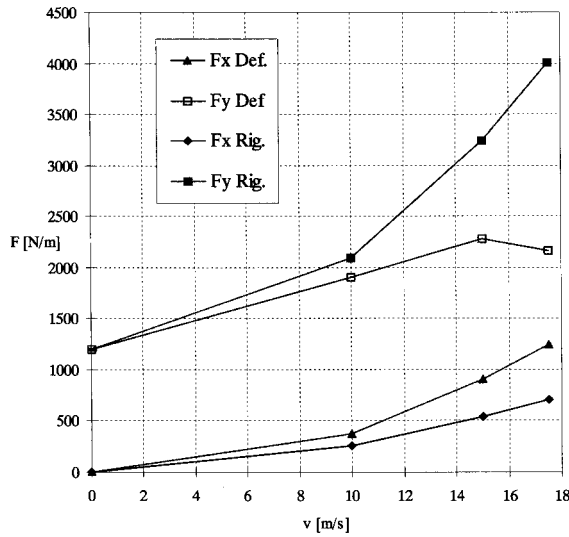


Fig. 8 Horizontal and vertical components of the resulting force on the membrane supports

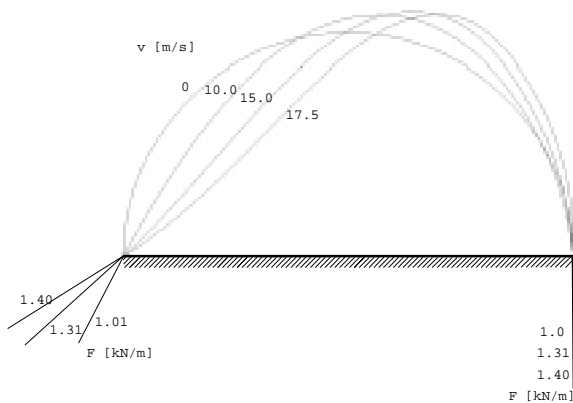


Fig. 9 Reaction forces to the supports and shape of the deformed membrane with respect to free stream velocity

Figure 10 presents the pressure distributions along the membrane. The position of the minimum pressure moves downstream with increasing velocity. Although the shape of the deformed membrane is far from cylindrical the difference between minimum pressures for flow around the deformable membrane and the ideal flow around the cylinder is -2.3 % for case 1, 1.5 % for case 2 and 2 % for case 3. On the back side of the

deformable membrane, the pressure distributions do not agree with the pressure distributions of the ideal flow around the cylinder. The result is the flow separation and a viscous loss in the whirlwind behind the membrane.

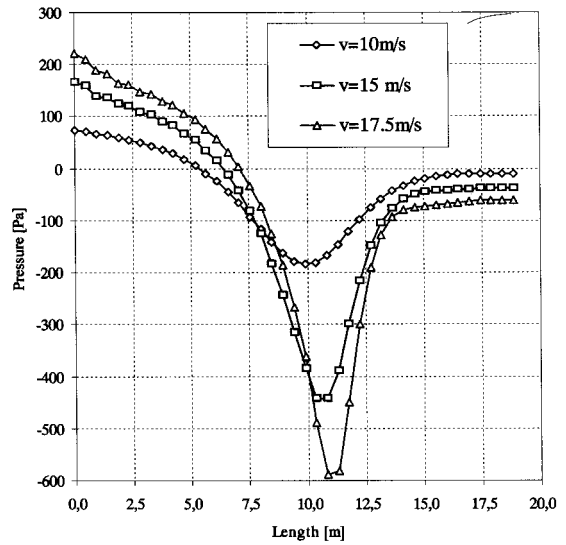


Fig. 10 Pressure distribution along the membrane surface

## 5. CONCLUSION

This paper deals with numerical modeling of a fluid-solid interaction problem. Some basic theoretical equations were presented in the first part while the second part deals with the modelling the wind force on the inflated membrane. In order to solve this problem the finite element method was used. Numerical analysis was performed in iteration cycles which consisted of calculating the flow field and calculating the deformation of the solid. The calculations were repeated until the static equilibrium of the solid was achieved. For the calculation of the solid deformation, nodal forces were defined which were not changed during the iteration. This led to an increased number of the global fluid-solid iterations which are still acceptably under 10.

The deformation of the membrane is tolerable for the pressure ratio less than 1.0. The membrane collapses for the pressure ratio exceeding 2.0. The wind flow horizontal force on the deformable membrane increases with the wind speed but the vertical forces attain a maximum between the wind velocities of 15 m/s and 17.5 m/s. Also the deformable membrane attains a maximum height between the wind velocities of 15 m/s and 17.5 m/s.

For calculating a dynamic solid-fluid interaction the fluid equations have to include non-stationarity and the solid equation mass acceleration. Also, the mass volume inside the membrane has to be considered. For the fluid description, the Euler-Lagrange formulation has to be used to fulfill the boundary condition in the interface between the fluid and solid.

## 6. REFERENCES

- [1] S. Cyr and B.G. Newman, Flow past two-dimensional membrane aerofoils with rear separation, *Journal of Wind Engineering and Industrial Aerodynamics*, Vol. 63, pp. 1-16, 1996.
- [2] K.L. Hedges, P.J. Richards and G.D. Mallison, Computer modelling of downwind sails, *Journal of Wind Engineering and Industrial Aerodynamics*, Vol. 63, pp. 95-105, 1996.
- [3] R. Smith and W. Shyy, Computation of aerodynamic coefficients for a flexible membrane airfoil in turbulent flow: A comparison with classical theory, *Physical Fluids*, Vol. 8, pp. 3346-3353, 1996.
- [4] J.H. Argyris, *Ta Panta Rei*, Elsevier Science Publisher B.V., 1985.
- [5] V. Šajn, Numerical modelling of a mechanical problem of solid-fluid interaction, M.Sc. Thesis, Faculty of Mechanical Engineering, University of Ljubljana, Ljubljana, 1996. (in Slovenian)
- [6] ABAQUS Version 6.2, Theory Manual, Hibbit Karlsson & Sorensen, Inc., 2002.
- [7] Fluid Dynamics Analysis Package - revision 8.6, Theory Manual, Fluid Dynamics International Inc., 2002.

## NUMERIČKA SIMULACIJA KRETANJA VJETRA OKO ELASTIČNE NAPUHANE MEMBRANE

### SAŽETAK

Cilj ovog rada je prikazati simulaciju turbulentnog kretanja vjetra oko elastične, napuhane cilindrične membrane. Aeroelastični model sastoji se od fleksibilne membrane s velikim pomacima i Navier-Stokes jednadžbe s Reynolds prosjekom nekog stacionarnog toka s  $k$ - $\epsilon$  modelom turbulencije. Kretanje vjetra oko membrane simulirano je kao dvo-dimenzionalni turbulentni tok oko krivulje koja se može deformirati i koja je pričvršćena na dva kraja. Za simulaciju ovog problema koristi se metoda konačnih elemenata. U iterativnom postupku proračuna oblik mreže fluida prilagođen je obliku krutog tijela. Ova prilagodba vrši se tako da se u procesu proračuna krutog tijela mreža fluida uzima kao slabo, skoro kruto tijelo. Simulacije su izvršene za brzine vjetra od 10, 15 i 17.5 m/s, a Reynolds brojevi u odnosu na promjer membrane od  $6.7 \cdot 10^6$ ,  $10 \cdot 10^6$  i  $11.8 \cdot 10^6$  s pritiskom napuhivanja od 100 Pa. Iz rezultata simulacije je vidljivo da je membrana stabilna i da ima prihvatljiv oblik kad je odnos između dinamičkog pritiska vjetra i untrašnjeg pritiska  $r_p$  manji od 1, dok se membrana ruši kad ovaj odnos pređe 2.

**Ključne riječi:** membrane, aeroelastičnost, interakcija fluid-kruto tijelo,  $k$ - $\epsilon$  model turbulencije.